Oxygen Permeability Measurements on Elastomers at Temperatures up to 225 °C

M. Celina* and K. T. Gillen

Sandia National Laboratories, Albuquerque, New Mexico 87185-1411

Received June 17, 2004; Revised Manuscript Received January 13, 2005

ABSTRACT: Oxygen permeability data, vital parameters for understanding and modeling the thermooxidative degradation of polymers, have been determined for various elastomers. Using a novel experimental setup, oxygen permeability through sheet materials was measured for elevated temperatures up to 225 °C. Under these conditions oxygen can react with the polymer reducing the effective O_2 flux. Knowing the relevant oxidation rates makes it possible to correct the permeability measurements for thermal oxidation occurring during permeation. A theoretical model using iterative data processing to determine true permeability data was developed to compensate for the oxidative loss of oxygen. The applicability to data collection and mathematical treatment for a range of materials is demonstrated. All permeability measurements exhibit curvature for an Arrhenius plot with activation energies being highly dependent on temperature.

1. Introduction

The performance and thermal aging of rubber materials with the aim of understanding their aging characteristics and developing appropriate lifetime prediction approaches are of ongoing interest to the polymer degradation community.[1−8] A major milestone in the mechanistic description of aging phenomena and accelerated degradation studies has been the demonstration and recognition that for oxidative environments diffusion-limited oxidation (DLO) effects at elevated temperatures or under other rate-determining aging conditions (photooxidation) can be highly important and need to be considered.[1−12] DLO effects can lead to complications via nonuniform bulk property changes and thus can misguide the various analyses used for a comprehensive description of the degradation.[2−4] Under high-temperature aging conditions where oxidation in the material consumes oxygen faster than it can be supplied via diffusion (permeation), heterogeneous oxidation profiles with more intense surface degradation (oxidation) will often result.[11,13] Edge effects and an arbitrary assessment of damage or "assumed" performance under these accelerated aging conditions can simply lead to wrong lifetime prediction scenarios. It is absolutely necessary to consider and understand DLO effects when conducting accelerated aging experiments.[2,3] A detailed understanding of such DLO effects and appropriate modeling requires knowledge of oxidation rates and oxygen permeability at elevated temperatures.[10,11] Sensitive oxygen consumption experiments[14] have been the key to measure the oxidation rates for many materials over large temperature ranges and have been used for predictive purposes.[1−4,14] The integrated oxidative damage often shows nonlinear Arrhenius behavior (based on comprehensive data superposition methodologies), leading to major implications for lifetime prediction approaches by challenging overly optimistic extrapolations when relying only on limited high-temperature aging data.[1,3,4]

* Corresponding author: Ph 505-8453551; fax 505-8449781; e-mail mccelin@sandia.gov.

Oxidation rate ϕ and oxygen permeability P (the product of diffusivity D and solubility S) are the two major parameters required to describe the aging and development of DLO profiles at elevated temperatures.[10,11] Low-temperature oxygen permeability data are available in the literature for some materials.[15,16] Some limited elevated temperature measurements have been conducted, but no detailed studies of the oxygen permeability in polymeric materials (rubbers) at high temperatures have been reported. The major problem when measuring permeability rates or oxygen flux is the unavoidable complication that a fraction of the oxygen will react with the material (oxidation) during the permeation process itself, particularly at higher temperatures. Any precise measurement of the total O_2 flux needs to be corrected for the O_2 fraction that is lost (consumed) during its path through the material. We are not aware of any studies that have ever considered the complexity of oxygen permeation in oxidation-sensitive materials such as rubbers at high temperatures. This paper is an attempt to establish the basis for such phenomena by measuring permeability rates and correcting the data for oxidation effects. Permeability measurements for a range of materials over different temperature ranges are presented.

2. Experimental Section

2.1. Permeability Apparatus and Measurements. Oxygen permeation experiments were performed on sheet samples (thickness is material dependent) using a custom-modified commercial Oxtran-100 coulometric permeation apparatus (Modern Controls, Inc., Minneapolis, MN). The instrumental setup is based on ASTM D3985-81.[17] The modified permeation chamber holding the sheet sample allows for permeation through a disk of approximately 64 mm diameter and is positioned in a common temperature-controlled laboratory oven to allow high-temperature experiments. The feed gas composition can be adjusted to any O_2/N_2 mixture between 100% N_2 and 100% O_2. The gas flow that collects the O_2 after diffusing through the sample contains ~2% H_2 (balance N_2). The actual concentration analysis relies on a reaction between O_2 and H_2 utilizing a proprietary catalysis-based sensor and thus is detected as a signal based on heat generation. As a further modification to the commercial instrument, we have included a bypass arrangement to quantitatively reduce the

10.1021/ma0487913 CCC: $30.25
Published on Web 02/22/2005

Table 1. Permeability Conversion Factors

conversions (76 cmHg = 101325 Pa)	cm^3 (STP) cm cm^{-2} s^{-1} $cmHg^{-1}$	cm^3 (STP) cm cm^{-2} s^{-1} Pa^{-1}	cm^3 (STP) cm cm^{-2} s^{-1} bar^{-1}
cm^3 (STP) cm cm^{-2} s^{-1} $cmHg^{-1}$	1	7.5×10^{-4}	75
cm^3 (STP) cm cm^{-2} s^{-1} Pa^{-1}	1333	1	10^5
cm^3 (STP) cm cm^{-2} s^{-1} bar^{-1}	0.01333	10^{-5}	1

percentage of the gas flow that reaches the detector. This allows for better measurements at elevated temperatures when O_2 permeation can be significant and could easily overload the sensor unit.

2.2. Oxygen Consumption (Uptake) Measurements. The consumption of oxygen as well as the formation of CO_2 and CO during thermal aging was determined using gas chromatography (GC). Details of this approach have been described before, and the technique has been established as a routine analysis.[14] Known amounts of samples (sufficiently thin to avoid diffusion-limited oxidation) were sealed at room temperature in ampules of known volume with an initial O_2 pressure calculated to give ~15 cmHg at the relevant aging temperature. The containers were then aged for periods of times which led to consumption of approximately 30% of the initial O_2. This resulted in an average partial pressure during each aging exposure of ~13 cmHg O_2, which is roughly equal to ambient air conditions in Albuquerque. At each aging temperature, the same sample was used sequentially to obtain time-dependent results.

2.3. Materials. 2.3.1. Black Viton Rubber. Compression-molded sheets (~1.5 mm thick) of V747-75 Viton rubber were obtained from the Parker Seal Group, O-ring division. It is a proprietary formulation based on a hexafluoropropylene−vinylidene fluoride copolymer in an approximately 2:1 ratio and 15% carbon black and cured using an organic bisphenol with an organo-phosphonium salt accelerator.[18]

2.3.2. Black EPDM Rubber. The EPDM (ethylene−propylene−diene−monomer rubber material)[19,20] used in this study was obtained as compression-molded sheets of approximately 1.9 mm thickness from Burke Rubber Industries.[21] The formulation of this EPDM rubber, a typical commercial product used to manufacture O-rings and seals, is 100 parts Nordel 1440 (random terpolymer of ethylene (~51.5%), propylene (~45.5%), and 1,4-hexadiene (~3%)), 5 pph zinc oxide, 2 pph Flectol H antioxidant (polymerized 1,2-dihydro-2,2,4-trimethylquinoline), 12 pph dicumyl peroxide (40% active), 10 pph SR-350 (trimethylol propane trimethacrylate) as an additional cross-linker, and 65 pph of carbon black (~34%) as a filler.[21]

2.3.3. Unfilled Neoprene Rubber. The neoprene ("polychloroprene") rubber material used in this study was also obtained as compression-molded sheets of approximately 2 mm thickness from Burke Rubber Industries. The formulation of this neoprene rubber, again a typical commercial product, commonly used to manufacture O-rings and seals, is 100 parts Neoprene GN, 5 pph zinc oxide, 4 pph magnesium oxide, 2 pph Vanox MBPC antioxidant (2,2′-methylenebis(4-methyl-6-*tert*-butylphenol)), 1.5 pph sulfur, 1.5 pph Altax cross-linker (2,2′-benzothiazolyl disulfide), and 0.5 pph stearic acid. This formulation does not include the usual ~40% hard-clay filler[11] but was thermally cured using the same procedure as normally applied to the filled material.

2.3.4. Unfilled Polyurethane Rubber. The polyurethane (PU) rubber investigated is a cured hydroxy-terminated polybutadiene (HTPB)/isophorone diisocyanate (IPDI) polymer. Samples of the uncured resins were provided by industry (Elf Atochem and Hüls America Inc.). Both components were mixed in a 1.0 molar reactivity ratio and include 1% Vanox MBPC antioxidant (2,2′-methylenebis(4-methyl-6-*tert*-butylphenol) in the HTPB.[4] The resulting resin was thermally cured for 1 week at 65 °C to obtain sheets of 2 mm thickness using Teflon-coated molds to allow for removal after curing.

2.3.5. Filled Polyurethane Rubber. A filled polyurethane binder was prepared to simulate a heavily loaded solid propellant material. The binder was filled with 20% fine aluminum powder and 68% KCl particles that would yield an "inert propellant" simulating a common aluminum/ammonium perchlorate-based system.

Table 2. Guidelines for Variations in *P*, *D*, and *S* for Different Gases in Polymers[15]

gas	*P*	*D*	*S*
N_2	1	1	1
O_2	3.8	1.7	2.2
CO_2	24	1	24
CO	1.2	1.1	1.1
He	15	60	0.25

3. Theoretical Background

3.1. Permeability through Polymers and Elastomers. Gas permeability P through a polymer film/sheet is defined as the gas volume (reduced to normal conditions) that passes through a polymer film of unit thickness, per unit area, per second, and at a unit pressure difference [cm^3 (STP) cm cm^{-2} s^{-1} $cmHg^{-1}$ or cm^3 (STP) cm^{-1} s^{-1} $cmHg^{-1}$]. Permeability P is the product of diffusivity D [cm^2 s^{-1}] and solubility S [cm^3 (STP) cm^{-3} polymer $cmHg^{-1}$] with common units for the permeability constant and conversions given in Table 1.[15]

Permeability of O_2 in polymers is normally higher than that of N_2. An approximate guideline (rule of thumb) on expected variations in permeability (P), diffusivity (D), and solubility (S) is given in Table 2.[15]

For most elastomeric polymers O_2 permeability constants at RT are expected to lie between $\sim 4 \times 10^{-11}$ and 5×10^{-8} cm^3 (STP) cm^{-1} s^{-1} $cmHg^{-1}$. Nitrile or butyl rubbers are expected at the lower range with natural rubbers or EPDM in the middle and silicone rubbers at the top of the permeability range. For semicrystalline materials there is a considerably larger variation, and as an example N_2 permeabilities between $\sim 10^{-13}$ and 10^{-8} cm^3 (STP) cm^{-1} s^{-1} $cmHg^{-1}$ at RT have been reported with fluorinated polymers, polyimides, or polyesters at the lower range.[15]

Some early data on the temperature dependence of gas permeability for some natural and butyl rubbers were presented in Arrhenius-type log(P) vs $1/T$ plots. Data were obtained over a temperature range of ~20−100 °C. The results showed curvature to lower E_a as T increased for the permeability and diffusivity of N_2 and low molecular weight alkanes in natural rubbers, but straight lines for the butyl material.[22] Similar curvature over ~20−100 °C was observed for He and N_2 permeation through a nitrile and natural rubber material.[23] In a more theoretical approach it was suggested that the activation energies for diffusivity in elastomers might be governed by segmental motion determined by the free volume of a polymer. This analysis predicts curvature to lower E_a's as the temperature increases consistent with the above experimental data.[24]

3.2. Oxidation Sensitivity of Polymers. During thermal exposure oxygen will react with most polymers leading to oxidation. The relevant oxidation rates can be conveniently measured with sensitive "oxuptake" or "oxygen consumption" methods. While simple measurements using pressure transducers can provide some

guidance on oxidation sensitivities, a better and more precise analytical method is gas chromatography (GC).[14,25] The advantage of this approach is that GC not only provides data on oxygen consumption but also on the formation of CO_2 and CO during thermal aging. Details of this approach have been described before, and the technique has been established as a simple routine analysis.[14] Samples are progressively aged at different aging temperature, providing time-dependent oxidation rates. The determination of oxidation rates and, when integrated with time, relative extents of oxidation or total oxygen consumed has been shown to allow for detailed superposition analyses describing the cumulative thermal aging at different temperatures.[1,3,4,14] This approach has been established as a useful methodology to aid the lifetime prediction of polymers.[1,3,4,14] For all the materials investigated in this permeation study we have determined the appropriate oxidation rates to be used in the numerical modeling as discussed later, either via direct measurements or simple inter- and extrapolations.

3.3. Theoretical Basis of Correcting O_2 Permeability Measurements for Loss of O_2 Due to Oxidation. The experimental arrangement for measuring oxygen permeability coefficients involves clamping a polymer sheet of uniform thickness L such that it separates an oxygen gas flow of oxygen partial pressure p on one side from a non-oxygen-containing gas flow on the opposite side. At equilibrium, a certain amount of oxygen will permeate through the sample thickness and will be detected on the opposite side. The rate of oxygen flowing through the material thickness is used to estimate the oxygen permeability coefficient. For convenience, we will assume that thickness is in the x-direction and that $x = 0$ corresponds to the surface exposed to oxygen and $x = L$ represents the side exposed to no oxygen flow. In normal circumstances where reaction of oxygen in the sheet during the permeation is unimportant, Fick's first law states that F_x, the oxygen flux in the x-direction per unit area in unit time, is proportional to the oxygen concentration gradient, that is

$$F_x = -D\left(\frac{\partial[O_2(x)]}{\partial x}\right) \tag{1}$$

where D is the oxygen diffusion coefficient through the material and $[O_2(x)]$ represents the oxygen concentration at location x. Under the measurement conditions described above, when steady state occurs

$$F_x = \frac{D[O_2(0)]}{L} \tag{2}$$

where $[O_2(0)]$ is the oxygen concentration at the oxygen-exposed surface of the sample. From Henry's law, $[O_2(0)]$ is given by the product of p the oxygen partial pressure at the surface and S the solubility coefficient for oxygen in the material. Combining this with eq 2 and noting that the permeability coefficient P is the product of D and S leads to

$$P = F_x\frac{L}{p} \tag{3}$$

In the absence of reaction under steady-state conditions, the flux F_x will be constant and independent of x-position or cross-sectional location. In other words, the steady-state oxygen concentration profile must be a straight line connecting the oxygen concentration $[O_2(0)]$ at $x = 0$ with $[O_2(L)] = 0$ as shown by the solid line (curve 1) in Figure 1.

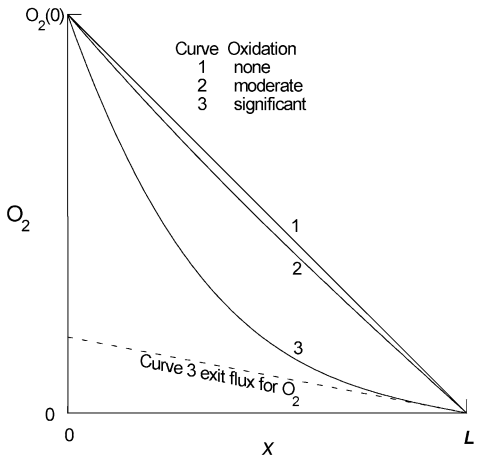

Figure 1. O_2 concentration profile through material of thickness L without and with loss of O_2 due to oxidation reactions. These modeling examples shown as curves 1, 2, and 3 relate to the neoprene material further discussed in section 4.4.

When oxidation is important, the oxygen flux will not be constant across the cross section since internal reaction implies that the flux (slope) entering the sheet must be greater than the flux (slope) exiting toward the detector. Thus, typical oxygen concentration profiles at steady state in such instances might be given by the solid curves (2 and 3) shown in Figure 1. From an experimental point of view, the detector will sense the flux exiting the sheet; this is represented for curve 3 in Figure 1 by the exit slope shown as the dashed line. In such cases the flux measurement will lead to incorrect values for P unless the measured flux is corrected for reaction effects. Modeling such corrections requires combining diffusion effects using Fick's law with chemical reaction expressions.[26,27] A very useful expression for the rate of oxidation of polymers was first derived in the 1950s[28−30] using the so-called basic autoxidation scheme (BAS) that involved an oxidation scheme encompassing three bimolecular termination reactions. The rate of oxidation was given by

$$\phi = \frac{d[O_2]}{dt} = \frac{C_1[O_2]}{1 + C_2[O_2]} \tag{4}$$

concentration profile through material of thickness L without and with loss of O_2 due to oxidation reactions. These modeling examples shown as curves 1, 2, and 3 relate to the neoprene material further discussed in section 4.4.

The constants C_1 and C_2 represent expressions involving the rate constants appropriate to the BAS bimolecular reaction scheme. We have shown previously that eq 4 also holds for other common variants of the BAS scheme, including unimolecular termination[10] and unimolecular termination in the presence of hydroperoxide branching reactions.[11] Since oxidation behavior consistent with eq 4 has been observed for many polymers,[4,5,10−12,18,31] we will model the reaction-modified permeation experiment utilizing this expression for the oxidation rate. Under steady-state conditions, the appropriate equation combining diffusion

with reaction then becomes[12,26]

$$D\frac{\partial^2[O_2(x)]}{\partial x^2} = \frac{C_1[O_2(x)]}{1 + C_2[O_2(x)]} \tag{5}$$

Using the following normalized variables for the x-axis and the oxygen concentration

$$X = x/L \qquad \theta = \frac{[O_2(x)]}{[O_2(0)]} \tag{6}$$

Equation 5 can be rearranged to the following expression

$$\frac{\partial^2\theta}{\partial X^2} = \frac{\alpha\theta}{1 + \beta\theta} \tag{7}$$

where the parameters α and β are given by

$$\alpha = \frac{C_1L^2}{D} \qquad \beta = C_2[O_2(0)] = C_2Sp \tag{8}$$

Equations 7 and 8 have been derived previously to examine diffusion-limited oxidation effects for polymers having planar geometry[11,12] where α and β are also related to the oxidation rate via eq 9.[11,12]

$$\frac{\phi L^2}{pP_{O_2}} = \frac{\alpha}{1 + \beta} \tag{9}$$

The solution approach involves dividing the interval X into k segments δX of equal length $1/k$ giving $k + 1$ points $j\delta X$ ($j = 0, 1, 2,..., k$). Calculating the oxygen concentration profile θ_j involves solving the following set of $k - 1$ simultaneous equations[12]

$$\theta_{j-1} = \frac{\alpha\theta_j(\delta X)^2}{1 + \beta\theta_j} + 2\theta_j - \theta_{j+1} \tag{10}$$

where $j = 1, 2, 3, ..., k - 1$. Since the oxygen concentrations at both sample surfaces are known ($\theta_0 = 1$ and $\theta_k = 0$ for the permeation sample), there are $k - 1$ equations and $k - 1$ unknowns (θ_1 through θ_{k-1}), allowing the unknowns to be evaluated by an iterative approach using eq 10. Previous uses of this approach utilized the derived oxygen concentration profiles to calculate the oxidation rate profiles from eq 4 to determine the importance of diffusion-limited oxidation. In the present application, however, we are concerned over the reduction in flux caused by oxidation reactions occurring in the permeability sample. Therefore, we are interested in the oxygen flux on the nitrogen-flowing side of the sample that is given by the slope of the oxygen concentration at this surface. For large enough values of k (we model using $k = 50$), this slope, defined as F (flux reduction factor) is given by

$$F = \frac{\Delta y}{\Delta x} = \frac{\theta_{k-1} - \theta_k}{1/k} = \theta_{k-1}k \tag{11}$$

Since normalized variables will lead to a slope of unity when reaction is unimportant, F represents the reduction in permeation flux caused by the reaction. Modeling results for the reduction in flux caused by reaction are shown in Figures 2 and 3 as a function of the variables α and β.

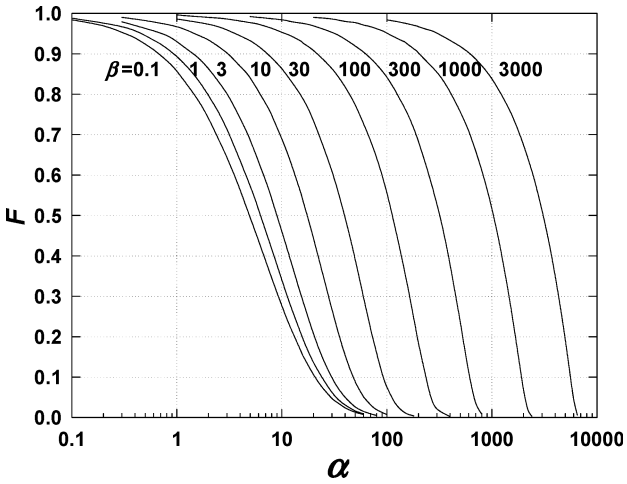

Figure 2. Model relationships between F and α for different values of β.

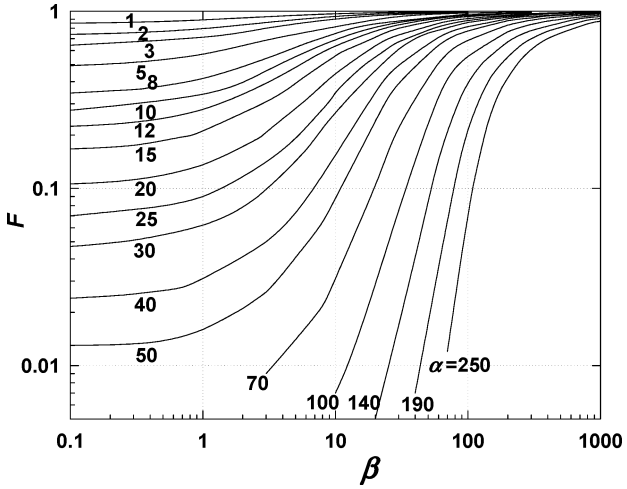

Figure 3. Model relationships between F and β for different values of α.

3.4. Iterative Solution To Obtain Corrected High-Temperature Permeability. We have developed an iterative approach to determine the real permeability (corrected) when some O_2 is lost due to oxidation at higher temperatures. Our iterative data analysis requires knowledge of the oxygen consumption rate at the measurement temperature and a value for β_{air}, a factor that combines rate constants, solubility, and O_2 partial pressure (see eq 8) and which essentially describes the sensitivity of oxidation rates on O_2 pressure.[11] First of all, the instrument detector will deliver a signal which when multiplied with an instrumental constant k_I (relating the detector signal to oxygen flux) gives the O_2 flux in cm^3 (STP) s^{-1} cm^{-2} of disk area. The apparent permeability P_{app} (uncorrected for reaction) is given as the product of k_I times the experimental flux times the sheet thickness L (cm) divided by the oxygen partial pressure differential across the sample Δp (cmHg).

$$P_{exp} = \frac{k_I \times \text{detector signal} \times L}{\Delta p} \tag{12}$$

The atmospheric pressure in Albuquerque is ~63 cmHg, implying that Δp will be given by the percentage oxygen flowing on one side of the sample times 0.63 cmHg. For a simple permeability measurement (as discussed in Figure 1 where $[O_2(L)] = 0$) Δp thus equals the oxygen

partial pressure (p_{O_2}) in the oxygen-exposed side of the sample. The actual value of the permeability will be the apparent value divided by the flux reduction factor F_i (Figures 2 and 3) or

$$P_i = \frac{P_{app}}{F_i} \tag{13}$$

In our iterative procedure, we initially assume no correction so that our initial estimate ($i = 1$) is $F_i = 1$. To obtain the values of α and β needed for correcting the permeability for reaction, we require oxygen consumption results ϕ (units of mol/(g s)) at the temperatures of interest to the permeability measurements. These are obtained using a technique that has been described in detail in previous publications.[1,14] The β value depends on β_{air}, which needs to be experimentally determined or often can be estimated for the material analyzed. For example in previous studies we have found that β_{air} for many elastomers under air-aging conditions ranges between ~0.5 and 5. Also, as will be shown below, the corrections for reaction are relatively insensitive to values of β_{air} in this range. Since β is linearly proportional to the oxygen partial pressure (eq 8), values of $\beta_{x\%}$ corresponding to $x\%$ O_2 will be given by

$$\beta_{x\%} = \frac{\beta_{air} \times x\%\ O_2}{20.95\%} \tag{14}$$

Equation 9 can now be used to estimate the initial value of α from

$$\alpha_i = \frac{\phi(\beta_{x\%} + 1)L^2 \times 22400\rho}{P_i \Delta p_{O_2}} \tag{15}$$

where ρ is the density of the sample in g/cm^3. Using the values of α and β obtained from eqs 14 and 15 leads (Figures 2 and 3) from the theory to an improved value of F_i ($i = 2$), which is then used in eq 13 to get an improved value of P_i to use in eq 15. After a few iterations, the results converge to give the corrected value of the oxygen permeability.

4. Oxygen Permeability of Different Rubbers

We present detailed permeability measurements obtained over a wide temperature range for different materials and at different O_2 partial pressures. Some materials show significant complications at the higher temperatures with oxidative reactions reducing the observed permeability. In general, whenever identical permeability data are obtained, independent of the O_2 partial pressure used for the experiments, oxidative reactions will be insignificant. A variation in permeability data for different O_2 partial pressures is an immediate indication of important oxidation reactions. In this case, the modeling scheme outlined above should reduce the different data to only one permeability (the material property P) at any given temperature. A consistent permeability result is in itself compelling evidence for the applicability of the model. When the reduced flux approaches ~10% (i.e., 90% reduction in O_2 flux due to oxidation), internal error margins in the mathematical treatment will increase and corrections would be too ambitious.

4.1. Oxidative Degradation (Material Changes) during Permeation Measurement. Recognizing that oxidation reactions at elevated temperatures will result in complications for permeability measurements immediately raises an important concern. Oxidative degradation during the experiment may in fact be sufficiently important, leading to significant material changes, which in turn could result in any permeability measurements not indicating the true material property but rather the permeability of an oxidized elastomer. This situation could be further complicated by DLO conditions where oxidative degradation is inhomogeneous, and material changes could develop faster near the oxygen-exposed surface. Obtaining meaningful permeability coefficients in this case would be virtually impossible. Therefore, experimental conditions need to be selected where the possibility of oxidation itself leading to changes in the material's oxygen solubility and/or diffusion coefficients has to be minimal.

Experimental conditions were chosen such that little oxidation occurs during the permeability measurements. The experimental procedure involved waiting at each measurement temperature until a steady-state flux was obtained. At high temperatures where oxidation effects become important, the high permeability values resulted in steady-state conditions being achieved in typically less than 1 h. The usual procedure was to obtain this "1 h" measurement, then wait, and take another measurement after another hour. The results from such time-dependent measurements were always very similar, showing no time dependence for all materials studied except at the highest temperature for the polyurethane (section 4.5). If important oxidation effects were occurring, one would expect the flux to change with time (extent of oxidation). Another approach to assess the issue of oxidative material changes both during and after the experiments is based on a comparison with thermooxidative damage in other properties. After the permeability experiments were completed, it was possible to compare the time scales required for the high-temperature measurements with time-dependent degradation data (e.g., tensile elongation, modulus, density) to further confirm that the measurements were completed before any significant degradation occurs in the material. Below are a few examples to substantiate our claims that permeability measurements on the chosen materials are taken when no changes in mechanical properties, and therefore significant oxidative damage, have occurred. Similarly, if significant oxidative changes occurred during the experiments, then the measurements should also depend on the thickness of the elastomer specimen. No differences between a 1 or 2 mm thick sheet were observed. Obviously, at very high oxidation rates (i.e., the highest temperatures investigated) it will be advantageous to use thinner films to minimize overall loss of O_2 in the material. This could enable some measurements that may not be possible on thicker materials.

For the Viton elastomer the oxidation rates are so low in any case that the oxygen flux for permeability measurements is not even affected. Mechanically, this material does not change. The data immediately yield true permeability. Model corrections are not required. For the EPDM material, the corrections in permeation occur in the temperature range of ~155−175 °C. Below are plots (Figures 4 and 5) demonstrating the measured changes at 155 and 170 °C for the elongation, density,

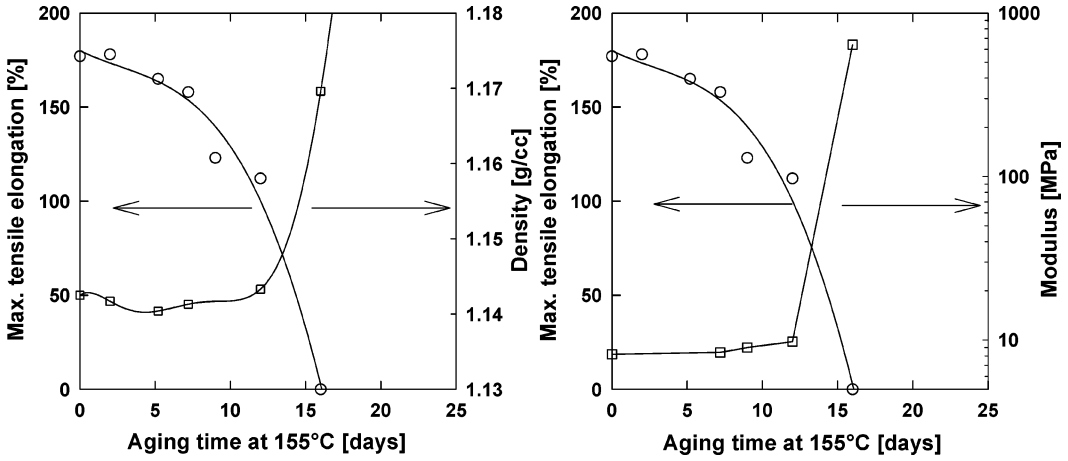

Figure 4. Changes for the EPDM material during thermal aging at 155 °C.

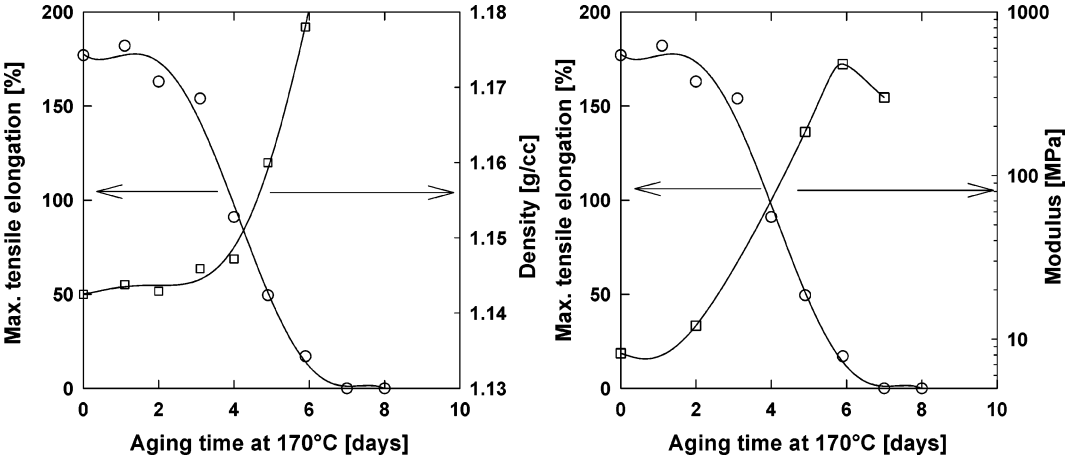

Figure 5. Changes for the EPDM material during thermal aging at 170 °C.

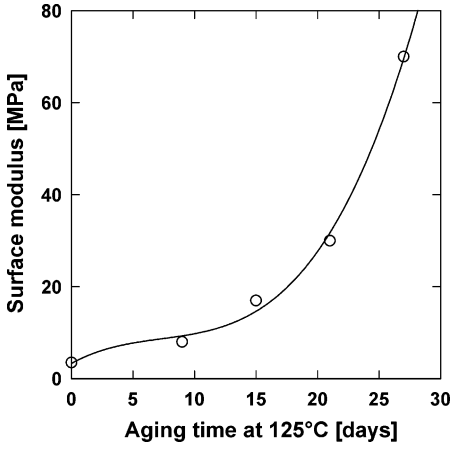

Figure 6. Hardening changes for the neoprene material during thermal aging at 125 °C.

and modulus that clearly show that, during the time required to obtain the permeation results (hours at most), little overall oxidative degradation occurs. No changes are expected to occur in the solubility or diffusion coefficient that could negatively affect permeability.

The neoprene material was analyzed with permeability fluxes corrected at temperatures from 95 to 125 °C. At the maximum temperature of 125 °C, it requires days before some limited modulus changes are observed (see Figure 6). Permeability measurements were taken over a few hours.

The only material and experimental condition, where some evidence of oxidation level dependent permeability measurements in this study were observed, are for the polyurethane material at the highest temperature, as discussed in section 4.5. In this case, measurements were taken up to 115 °C and were found to depend on the exposure time at this temperature, indicating that oxidation effects at this condition are important enough to cause changes in the short-term oxygen flux. This is the only example where it was apparent that thermal degradation had a minor effect on the permeability. A useful measurement could still be obtained via extrapolation of time-dependent data to time zero.

4.2. Viton. The O_2 permeability through a commercial black Viton material was analyzed from RT to ~225 °C. The apparent permeability data (uncorrected for possible oxidation effects) for different relative O_2 partial pressures (air, 50%, and 100%) are shown in Figure 7 and yield identical permeability at all the temperatures investigated for each O_2 partial pressure. This material has a relatively low permeability at the lower temperatures, consistent with the current data on fluorinated materials.[15] No effect of O_2 partial pressure is apparent for the high-T data, suggesting unimportant oxidation effects as expected for a highly fluorinated material. Of interest is to note the significant curvature in the Arrhenius plot of the permeability vs inverse temperature data consistent with earlier literature and modeling results.[22−24]

4.3. EPDM. The O_2 permeability for a commercial black EPDM material was analyzed from RT to 175 °C.

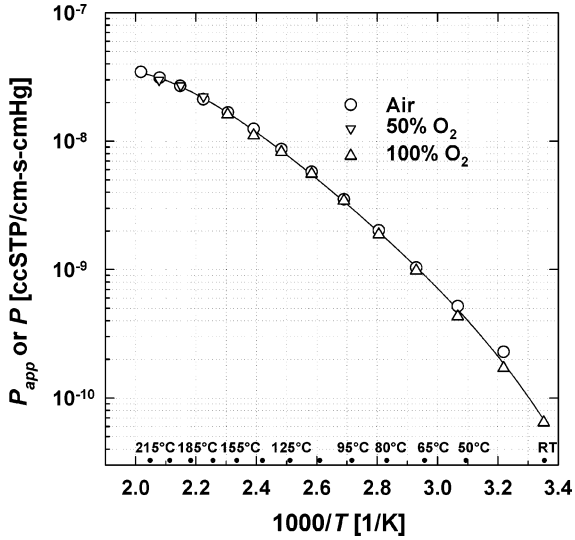

Figure 7. Permeability of O_2 measured at various O_2 partial pressures through a Viton sheet sample measured at temperatures of up to ~220 °C. No corrections for oxidation are necessary.

The apparent permeability data were measured for different O_2 partial pressures (10.5%, air, and 50%), as shown in Figure 8a. Permeability values with important dependence on % O_2 are observed only for temperatures above ~150 °C. At the highest temperatures we see evidence for a maximum in the apparent permeability and an O_2 partial pressure dependence with the lowest O_2 concentration of 10.5% yielding the lowest permeability. These observations suggest that not all of the available oxygen reaches the detector. Using previously measured data for the oxidation rates[31] allows to correct the apparent permeability for oxidative loss with the iterative approach discussed above. Each individual data point for the higher temperatures was corrected with the resulting corrected permeability values shown in Figure 8b. Lacking the precise value, we used β_{air} of 1 for the EPDM as a variable in these calculations. We will show for the next material (neoprene rubber) that iterative corrections are relatively insensitive to variations in β_{air}. All corrected permeability data now follow a single trend (Figure 8b), and permeability at the highest temperatures is larger than what the noncorrected data would suggest (Figure 8a). The EPDM material has an O_2 permeability (P) of $\sim 2 \times 10^{-9}$ cm^3 (STP) cm^{-1} s^{-1} cmHg^{-1} at 25 °C in the range expected for such materials.[16] In agreement with our measurements for the Viton material, we also observe a curvature in the Arrhenius plot of corrected permeability vs inverse temperature.

4.4. Neoprene. The O_2 permeability for an unfilled (no clay filler) neoprene rubber material (polychloroprene elastomer) was measured from RT to 135 °C. The apparent permeability data for different O_2 partial pressures (10.5%, air, 50%, and 100%) are shown as obtained in Figure 9a. Depending on the chosen O_2 concentration, different permeability results are observed at temperatures of 60 °C and above. Lower O_2 concentrations yield lower apparent permeability, and most importantly we observe a maximum in the observed permeability at ~105 °C with a pronounced reduction in P_{app} when carrying out measurements at even higher temperatures (Figure 9a). This is clearly a situation where the permeability is influenced by important oxidation effects. Most of the available oxygen is consumed during the permeation process, and a crude estimation (extrapolation of low-T data) of the actual O_2 flux at the highest temperature (135 °C) indicates that on the order of only ~10% of the O_2 may reach the detector. The reduction in P_{app} is much more pronounced than that observed for the EPDM sample.

Again, using previously measured data for the oxidation rates[5] and the same iterative approach provides the basis to correct the permeability for oxidative loss. Each individual datum point for the higher temperatures was corrected for oxidation leading to the data shown in Figure 9b. For these permeability corrections we used a β_{air} of 0.7, which was previously found to be appropriate for a filled neoprene.[11] However, further modeling calculations demonstrated that the corrections are rather insensitive to β_{air} over the range of reasonable values of β_{air} ($0.2 < \beta_{air} < 2$). This is apparent in Figure 9b where even at the highest temperature analyzed (~125 °C) there is only a small variation over the range of β_{air} values. It was not possible to correct the original measurements taken at ~135 °C, since the actual O_2 flux is too low (≤10%) for the iterative correction process to deliver a reasonable number. Such low fluxes may represent the limit for the modeling. In summary, all permeability data superpose to a single curve (the data in Figure 9b represent the averages obtained from the different O_2 concentrations), and the corrected permeability P at the higher temperatures is considerably larger than the noncorrected apparent data as shown in Figure 9a. The neoprene has an O_2 permeability of $\sim 4 \times 10^{-10}$ cm^3 (STP) cm^{-1} s^{-1} cmHg^{-1} at ambient temperature, considerably lower than the EPDM material. Curvature in the corrected permeability P vs inverse temperature data is also apparent.

The corrected experimental permeability data determined for this material served as the basis to model the schematic O_2 profiles presented earlier in Figure 1. These curves were modeled using measured oxidation rates (ϕ),[5] corrected permeability data P, β_{air}, and α values calculated using eq 15, with the modeling parameters for the three curves summarized in Table 3. They demonstrate the expected equilibrium conditions in a 2 mm thick neoprene material for different experimental conditions (see Figure 1).

4.5. PU Binder. The O_2 permeation for an unfilled polyurethane material (HTPB/IPDI based) was analyzed from RT to 115 °C. This material is used as a binder for inorganic-based propellants, and its aging in terms of oxidative degradation is of interest in current studies.[4,32] As before, experiments were carried out for different O_2 partial pressures (10.5%, air, 50%, and 100%) with the apparent results (P_{app}) shown in Figure 10a (data as measured). Similar to the neoprene sample, we observe a dramatic decrease in apparent permeability at temperatures larger than ~85 °C. This represents another nice example of a material where oxidation at elevated temperatures is considerable, and appropriate corrections for oxidative loss are required to yield meaningful permeability data. Oxygen consumption rates for this material have been determined in great detail, and extensive consumption rate vs O_2 pressure measurements resulted in the determination of β_{air} as ~10 for this material.[4,32]

Using the known oxidation rates, our iteration process yielded the corrected permeability data shown in Figure 10b. Initial corrections, however, resulted in lower than expected data that did not seem to follow the same

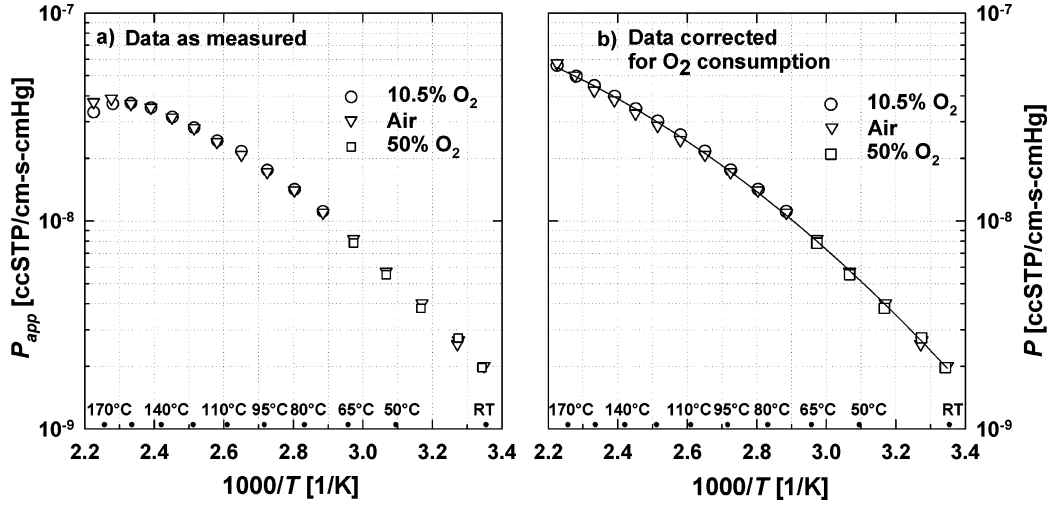

Figure 8. (a) Apparent permeability of O_2 measured at various O_2 partial pressures through an EPDM sheet sample measured at temperatures of up to ~180 °C. (b) Permeability values corrected for reaction losses.

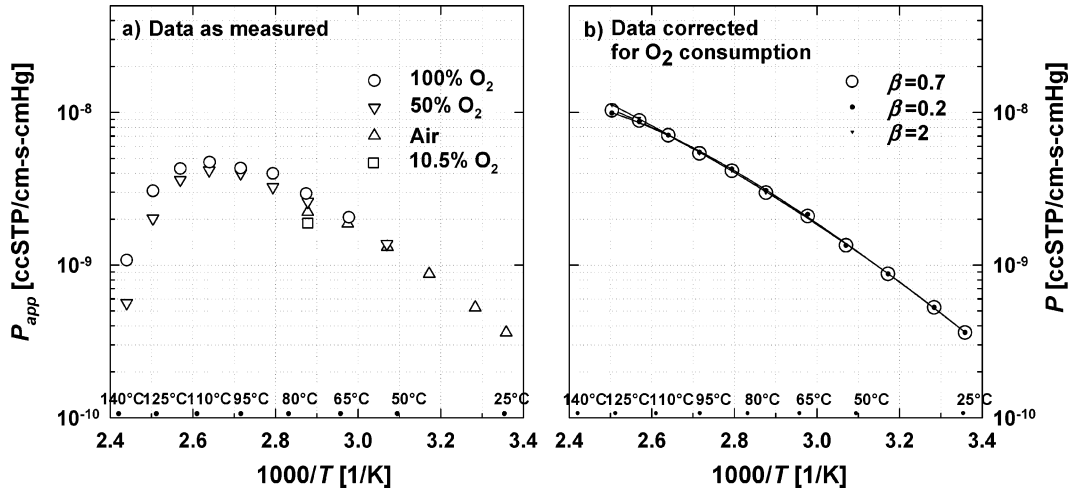

Figure 9. (a) Apparent permeability of O_2 measured at various O_2 partial pressures through a Neoprene sheet sample measured at temperatures of up to ~125 °C, showing significant loss of O_2 at the higher temperatures due to oxidation. (b) Corrected permeability for different β_{air} values.

Table 3. Parameters Used for Modeling Oxygen Concentration Profiles Shown in Figure 1

curve	T [°C]	p_{O_2} [cmHg]	ϕ [mol/(g s)]	P [cm^3 (STP) cm^{-1} s^{-1} cmHg^{-1}]	β	α
1	RT	13.2 (air)	1.0×10^{-12}	3.6×10^{-10}	1	0.01
2	65	13.2 (air)	1.06×10^{-11}	2.2×10^{-9}	1	0.85
3	125	31.5 (50% O_2)	1.09×10^{-9}	1.0×10^{-8}	2.38	19.2

trends as observed for the other materials. We found that this material is somewhat unusual in that cumulative oxidation (total extent of oxidation) has an important impact on permeability itself (damage- or aging-dependent permeability as discussed in section 4.1). Oxidative damage, which becomes significant at the elevated temperatures, results in material hardening that leads to a reduction in oxygen permeability with time. Similar conclusions were presented when studying the thermal degradation and oxidation fronts in such materials with imaging chemiluminescence.[8] To minimize such oxidative damage effects, each air measurement above ~80 °C was carried out on a new sheet of the material. Additionally, we also monitored the time development of the permeability measurements. At least a few hours is required to allow for the first equilibrium measurement during which oxidative damage already occurs. By plotting measurements vs aging time, we were able to extrapolate the data to time zero. This procedure was carried out for the air measurements at the four highest temperatures. The zero-time extrapolated data are included in Figure 10b as the dotted curve. Overall, this effect does not constitute a large correction when a new sample is used for each high-temperature analysis. However, it is important to consider the dependence of permeability on oxidative damage when carrying out repeated measurements on a single sheet of material. This polyurethane has a relatively high O_2 permeability of $\sim 3.5 \times 10^{-9}$ cm^3 (STP) cm^{-1} s^{-1} cmHg^{-1} at ambient temperature and similar curvature in the corrected permeability vs inverse temperature data as observed for the other materials.

4.6. PU Binder, Comparison of Unfilled and Filled Material. Of interest is to compare the permeability of the unfilled material with that of a sample containing inorganic particles. Such data are required for appropriate degradation modeling of filled materials.[4] The filled material was loaded with ~88% per weight aluminum powder and KCl particles. As shown in Figure 11, the corrected permeability of the filled

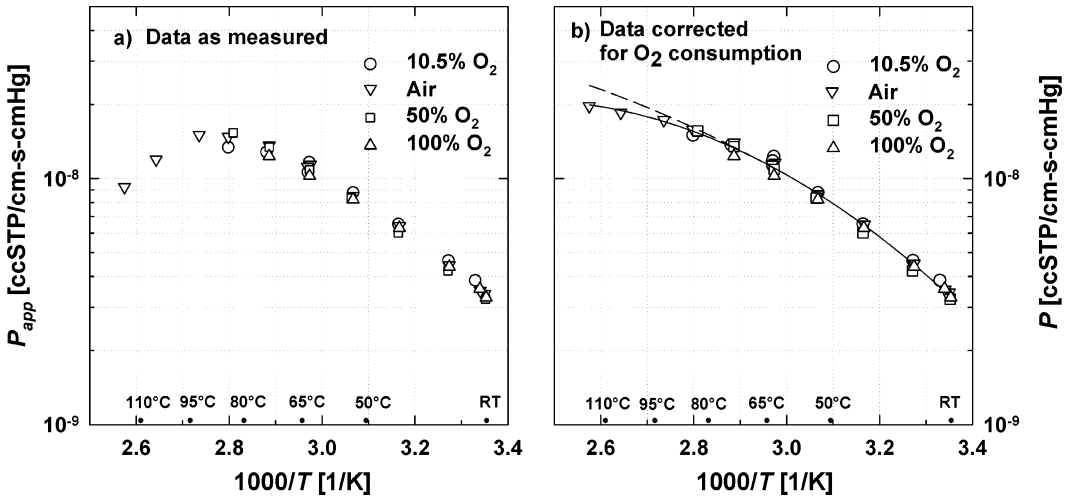

Figure 10. (a) Apparent permeability of O_2 measured at various O_2 partial pressures through a PU sheet sample measured at temperatures of up to ~125 °C showing significant loss of O_2 at the higher temperatures due to oxidation. (b) Corrected permeability values.

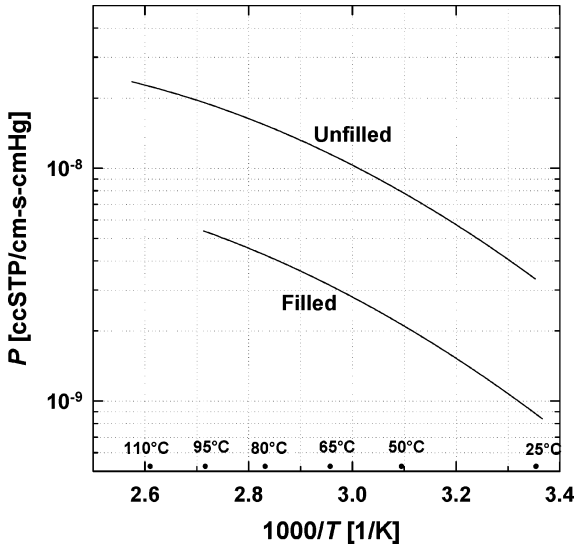

Figure 11. Comparison of O_2 permeability through an unfilled and filled PU sheet sample.

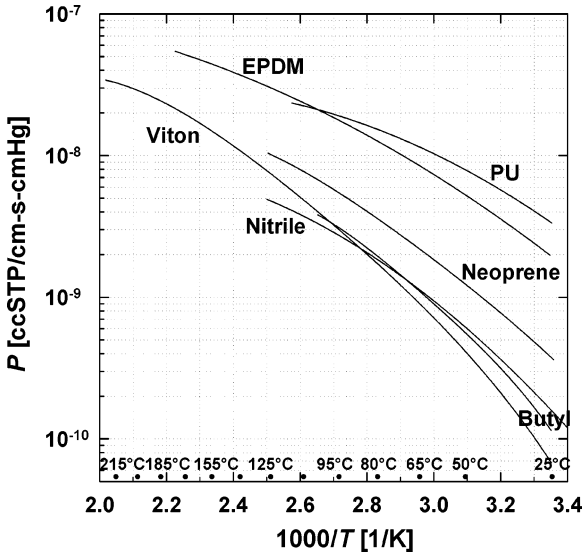

Figure 12. Comparison of O_2 permeability for different elastomers.

material is consistently lower, by a factor of approximately 4. This difference between the unfilled and filled material is difficult to predict. On a per volume basis the filled polymer has only approximately 23% polymer, and this would support a reduced permeability of 25%. However, permeability in filled polymer systems would not be expected to change with a linear dependence, as the permeability process is highly complex. Reduced permeability would result from an increase in permeation path length (tortuosity), but material imperfections and microvoids would act the opposite way. A simple tortuosity assessment predicts a lower permeability than that observed, which suggests that some imperfections in the filled material are present and would need to be considered.

4.7. Curvature in 1/*T* Plots and Activation Energies. For comparison purposes, the permeability data of the different materials investigated are summarized in Figure 12. This plot contains additional data of a black nitrile rubber that was previously analyzed[11] and data points for a commercial butyl rubber compound. A fundamental feature for all materials in this plot is the considerable curvature in the permeability vs 1/*T* data. Such curvature would not be readily apparent in many past permeability measurements that covered a more limited temperature range (e.g., RT to 60 or 80 °C). This can be seen by examining the corrected data from RT up to 60 or 80 °C in Figures 7, 8b, 9b, and 10b. Only the extended temperature range used in the current experiments makes the curvature obvious. As mentioned earlier, such curvature has been noted in earlier studies.[22−24]

The observed curvature implies that activation energies for permeability will be temperature dependent. This is best presented by plotting the derivatives of the Arrhenius permeation plots. Figure 13 shows how the activation energies E_{act} (see also Table 4) depend on temperature. Since permeability is the product of diffusivity and solubility, and considering that solubility can be regarded as more or less independent of temperature,[11,16] it is reasonable to assume that changes in diffusivity are primarily responsible for the observed temperature effect. For instance, for a filled nitrile rubber it was shown that oxygen solubility was unchanged with temperature, but diffusivity increased.[11] Similarly, literature data for numerous elastomers and other polymers show solubility to depend on temperature with activation energies of generally not more than

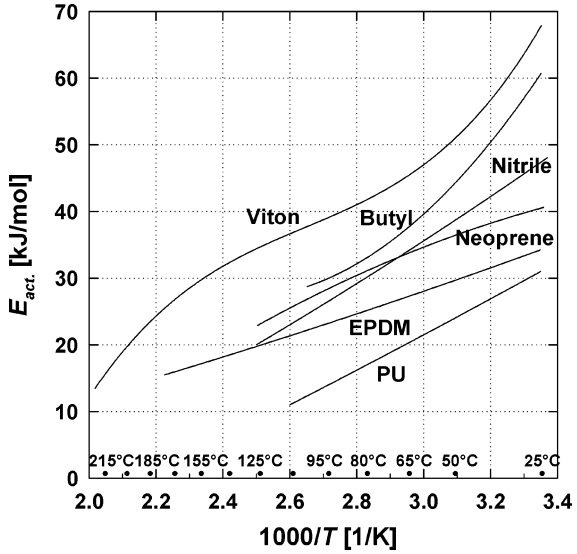

Figure 13. Temperature-dependent activation energies for the permeability data shown in Figure 12.

Table 4. Activation Energies for Low- and High-Temperatures Regimes

	E_{act} [kJ/mol] at low T		E_{act} [kJ/mol] at high T	
butyl	54.1	RT−40 °C	30.3	85−105 °C
EPDM	31.4	RT−50 °C	18.9	140−175 °C
neoprene	37.8	RT−50 °C	25.6	95−125 °C
nitrile	42.5	RT−50 °C	21.6	85−125 °C
PU binder	26.9	RT−50 °C	13.7	85−115 °C
Viton	56.2	RT−50 °C	17.4	175−220 °C

±10 kJ/mol.[16] Diffusivity changes should therefore closely track those observed in the permeability.

5. Conclusions

We have successfully carried out oxygen permeability measurements on different rubber materials over a large temperature range of up to 225 °C. Accurate measurements at elevated temperatures are often complicated by oxidation reactions occurring in the material. This partial O_2 loss results in lower effective O_2 fluxes and thus lower apparent permeability values. Knowing the relevant oxidation rates, we have established a model that compensates for such oxidative loss and yields corrected permeability data. This model uses iterative solutions based on oxidation rate, measured permeability, and other factors and is capable of yielding corrected permeability data when the total oxygen flux may be as low as 20% of the expected flux in the absence of oxidation reactions. All materials investigated show curvature in the Arrhenius plots of permeability vs inverse temperature. This demonstrates that activation energies are dependent on temperature.

Acknowledgment. Sandia is a multiprogram laboratory operated by Sandia Corporation, a Lockheed Martin Company, for the United States Department of Energy's National Nuclear Security Administration under Contract DE-AC04-94AL85000.

References and Notes

(1) Gillen, K. T.; Celina, M.; Clough, R. L.; Wise, J. *Trends Polym. Sci.* **1997**, *5*, 250.
(2) Gillen, K. T.; Celina, M.; Keenan, M. R. *Rubber Chem. Technol.* **2000**, *73*, 265.
(3) Gillen, K. T.; Celina, M.; Bernstein, R. *Polym. Degrad. Stab.* **2003**, *82*, 25.
(4) Celina, M.; Graham, A. C.; Gillen, K. T.; Assink, R. A.; Minier, L. M. *Rubber Chem. Technol.* **2000**, *73*, 678.
(5) Celina, M.; Wise, J.; Ottesen, D. K.; Gillen, K. T.; Clough, R. L. *Polym. Degrad. Stab.* **2000**, *68*, 171.
(6) Rincon-Rubio, L. M.; Colin, X.; Audouin, L.; Verdu, J. *Rubber Chem. Technol.* **2003**, *76*, 460.
(7) Stevenson, A.; Campion, R. *Engineering with Rubber*; Carl Hanser Verlag: Berlin, 2001; p 177.
(8) Sinturel, C.; Billingham, N. C. *Polym. Int.* **2000**, *49*, 937.
(9) Clough, R. L.; Gillen, K. T. *Polym. Degrad. Stab.* **1992**, *38*, 47.
(10) Gillen, K. T.; Clough, R. L. *Polymer* **1992**, *33*, 4358.
(11) Wise, J.; Gillen, K. T.; Clough, R. L. *Polymer* **1997**, *38*, 1929.
(12) Cunliffe, A. V.; Davis, A. *Polym. Degrad. Stab.* **1982**, *4*, 17.
(13) Gillen, K. T.; Terrill, E. R.; Winter, R. M. *Rubber Chem. Technol.* **2001**, *74*, 428.
(14) Wise, J.; Gillen, K. T.; Clough, R. L. *Polym. Degrad. Stab.* **1995**, *49*, 403.
(15) Krevelen, D. W. *Properties of Polymers*; Elsevier: Amsterdam, 1997; Chapter 18, p 535.
(16) Pauly, S. *Polymer Handbook*; J. Wiley & Sons: New York, 1999; Chapter VI, p 543.
(17) ASTM Standard D3985-81, Oxygen Gas Transmission Rate through Plastic Film and Sheeting Using a Coulometric Sensor.
(18) Wise, J.; Gillen, K. T.; Clough, R. L. *Radiat. Phys. Chem.* **1997**, *49*, 565.
(19) Borg, E. L. In Kirk R. E., Othmer, D. F., Eds.; *Encyclopedia of Chemical Technology,* 3rd ed.; J Wiley & Sons: New York, 1979; Chapter 8, p 515.
(20) Easterbrook, E. K.; Allen, R. D. In Morton, M., Ed.; *Rubber Technology*; Chapman & Hall: London, 1995; Chapter 9, p 260.
(21) Gillen, K. T.; Celina, M.; Clough, R. L.; Malone, G. M.; Keenan, M. R.; Wise, J. *Sandia Report SAND98-1942*; Sandia National Laboratories: Albuquerque, NM, 1998.
(22) Barrer, R. M. *J. Polym. Sci.* **1948**, *3*, 549.
(23) Amerongen, G. J. *J. Polym. Sci.* **1950**, *5*, 307.
(24) Kosiyanon, R.; McGregor, R. *J. Appl. Polym. Sci.* **1981**, *26*, 629.
(25) Scheirs, J.; Bigger, S. W.; Billingham, N. C. *Polym. Test.* **1995**, *14*, 211.
(26) Crank, J. *The Mathematics of Diffusion*; Clarendon Press: Oxford, 1970.
(27) Vieth, W. R. *Diffusion in and through Polymers*; Hanser Publishers: New York, 1991.
(28) Bolland, J. L. *Proc. R. Soc. London* **1946**, *A186*, 218.
(29) Bateman, L. *Q. Rev.* **1954**, *8*, 147.
(30) Bateman, L.; Gee, G.; Morris, A. L.; Watson, W. F. *Discuss. Faraday Soc.* **1951**, *10*, 250.
(31) Gillen, K. T.; Celina, M. *Polym. Degrad. Stab.* **2001**, *71*, 15.
(32) Celina, M.; Graham, A. C.; Gillen, K. T.; Assink, R. A.; Minier, L. M. *5th Life Cycles of Energetic Materials*, Orlando, FL, 1999; p 307.

MA0487913